The Influence of Pre-treatment Time and Sulfuric Acid on Cellulose Nanocrystals

Ya-Yu Li,[a,b,c] Bin Wang,[a] Ming-Guo Ma,[a,*] and Bo Wang [a]

Cellulose nanocrystals (CNCs) were produced with different pre-mixing times between the cotton fiber and the sulfuric acid at room temperature, prior to the reaction at 45 °C. The CNC0 and CNC60 films were prepared using vacuum filtration methods. Based on transmission electron microscopy observations, the dimension and yield of CNCs gradually decreased with increasing pre-mixing time. Considering the balance of yield and quality of CNCs, CNC0 was chosen as the optimal product. The synthetic process played an important role in the production of CNCs. Various CNCs had similar crystallinity index values with the increased pre-mixing time. The decreased contact angle was the result of decreased dimensions of CNCs or the additional sulfate group at the surface of the CNCs. Both thermogravimetric and contact angle analysis are sensitive for the constituents of CNCs.

Keywords: Cellulose nanocrystals; Sulfuric acid; Pre-mixing time; Characterization

*Contact information: a: Engineering Research Center of Forestry Biomass Materials and Bioenergy, Beijing Key Laboratory of Lignocellulosic Chemistry, College of Materials Science and Technology, Beijing Forestry University, Beijing 100083, PR China; b: College of Chemical Engineering, Xinjiang Agricultural University, Urumqi 830052, Xinjiang Province, PR China; c: Xinjiang Blue Ridge Tunhe Profiles Co., Ltd., Changji 831100, Xinjiang Province, PR China; * Corresponding author: mg_ma@bjfu.edu.cn*

INTRODUCTION

Cellulose nanocrystals (CNCs) have been developed for their distinct properties, *e.g*., biocompatibility, high elastic modulus (Wang *et al.* 2012; Zhang *et al.* 2016), high specific surface area (Huang *et al.* 2016; Li *et al.* 2017), distinct optical properties (Csiszar and Nagy 2017; Zhang *et al.* 2017), and high aspect ratio (Chen *et al.* 2015). CNCs have been added into matrix to prepare mechanically enhanced materials (Gawryla *et al.* 2009; Pei *et al.* 2011; Meesorn *et al.* 2017; Sapkota *et al.* 2017; Nicharat *et al.* 2017), mechanically-adaptive materials (Mendez *et al.* 2011; Way *et al.* 2012; Biyani *et al.* 2013; Biyani *et al.* 2014), self-healing materials (Imato *et al.* 2017), synthesis templates (Padalkar *et al.* 2010), biosensors (Schyrr *et al.* 2014), and so on. Sobolciak *et al.* (2017) modified co-polyamide nanofibers using CNCs and a one-step method from date palm leaves, which showcased the increased mechanical properties and hydrophilicity. Yan *et al.* (2017) prepared bacterial cellulose nanocrystals and verified their high thermal stability and good emulsifying performance compared with bacterial cellulose. Multifunctional composites with enhanced mechanical strength and antibacterial properties were prepared by melt extrusion of three components including poly(lactic acid), CNC, and silver nanoparticles in food packages application (Fortunati *et al.* 2012). Shanmuganathan *et al.* (2010) introduced percolating networks of CNCs into polymer matrix as adaptive substrates for intracortical electrodes. When this nanocomposite was immersed into emulated physiological solution, its tensile storage moduli can be reduced significantly from 40 MPa to 5 MPa with only about 28% w/w swelling. Yu *et al.* (2017) obtained electrospun

composite nanofibers by adding CNCs/polyethylene glycol (PEG) to poly(lactic acid) (PLA). In comparison to neat PLA, the addition of CNCs/PEG reduced fiber diameters, enhanced fiber uniformity, and decreased the water contact angle (CA) of composite nanofibers with 10 wt.% CNCs/PEG from 117.3° to 98.0°.

There are various strategies to produce CNCs. Diluted sulfuric acid was firstly used for CNCs preparation in 1951 by Rånby. Concentrated sulfuric acid was determined to be a better option in CNC production by Mukherjee and Woods (1953), and actually their procedure is the precursor for the ubiquitous sulfuric acid method still in use today. Chieng *et al*. (2017) produced CNCs by H_2SO_4 acid hydrolysis of oil palm mesocarp fiber after the removal of hemicellulose and lignin. Sampath *et al*. (2017) prepared CNCs of approximately 200 nm to 300 nm in length and 40 nm to 50 nm in width from microcrystalline cellulose (MCC) *via* sulfuric acid hydrolysis. This process was used to fabricate CNCs-chitosan hydrogels with improved mechanical properties and pH sensitivity. The shape and size distribution of CNCs extracted from cotton, Avicel, and tunicate have been investigated comprehensively using transmission electron microscopy, atomic force microscopy, and X-ray scattering (Elazzouzi-Hafraoui *et al.* 2008). In addition to sulfuric acid hydrolysis method, Kontturi's group developed a hydrogen chloride acid vapor hydrolysis method followed by TEMPO oxidation towards more effortless isolation of cellulose nanocrystals (Kontturi *et al.* 2016; Lorenz *et al.* 2017; Lee 2018). Besides acid hydrolysis, Trache *et al.* (2017) summarized six categories of methods including mechanical treatment, oxidation method, enzymatic hydrolysis, ionic liquid treatment, subcritical water hydrolysis, and combined process.

There are several strategies to optimize the synthetic condition of CNCs using the sulfuric acid hydrolysis method. Beck-Candanedo *et al*. (2005) examined the effects of reaction time and acid-to-pulp ratio on nanocrystal and suspension properties for hydrolyzed black spruce acid sulfite pulp. They found that longer hydrolysis times produced shorter and less polydisperse black spruce CNCs. Bondeson *et al*. (2006) optimized the production of CNCs from MCC with a sulfuric acid concentration of 63.5% (w/w) and a reaction time of 2 h using response surface methodology. Ioelovich (2012a, b) reported the optimal conditions for obtaining CNCs and studied carefully the dissolution process of cellulose in various concentrations of sulfuric acid and temperatures. The study found that the optimal conditions of the acidic treatment for the isolation of CNCs were the sulfuric acid concentration of 57 wt.% to 60 wt.%, acid to cellulose ratio of 8 to 10, and temperature of 45 °C to 55 °C for 40 to 60 min.

The mechanism of sulfuric acid hydrolysis of cellulose is usually explained by selective acid hydrolysis of disordered (amorphous) domains of cellulose nano-fibrils; the more resistant nanocrystallites remain intact and can be isolated in a form of rod-like particles (Habibi *et al.* 2010). Camacho *et al*. (1996) analyzed the effects of temperature (25 °C to 40 °C), H_2SO_4 concentration (31% to 70% (w/v)), and the acid/substrate relationship (1 cm^3 to 5 cm^3 of H_2SO_4 per g of cellulose) on the solubilization rate of MCC and glucose production. They found that the solubilization followed zero-order kinetics and the production of glucose was a two part consecutive first-order pseudo-homogeneous reaction. Wang *et al*. (2014) used three phenomenological reactions to express the solubilization of cellulose fibers, which could be described by pseudo-homogenous first-order kinetics.

Nevertheless, the interaction between cellulose and sulfuric acid is not completely understood (Moon *et al*. 2011). For example, the process of hydrolysis of cellulose can be divided into two sequential processes, specifically of the solubilization and the

depolymerization of cellulose. The solubilization process of cellulose in sulfuric acid includes the swelling and dissolving of cellulose, meaning that the acid penetrates the noncrystalline and crystalline domains of cellulose and forms complexes (Ioelovich 2016). The depolymerization process means the decrease of degree of polymerization (DP) of cellulose macromolecular, particularly the decomposition of noncrystalline domains and finally, CNC is produced. Similar to the results of Camacho *et al*. (1996), these two processes may have different kinetics too. So at room temperatures and 45 °C, the relative rate of the two processes may vary. In order to verify the effect of this temperature assembly on yield and uniformity of CNC, the different pre-mixing times at room temperature prior to acid hydrolysis at 45 °C were implemented. This approach has not been reported yet. The purpose of this paper is to investigate the influences of pre-treatment with sulfuric acid prior to the hydrolysis. Herein, two levels of temperature were chosen, room temperature (~25 °C) and 45 °C, to investigate the effects of pre-mixing between cotton and sulfuric acid on the yield and properties of CNCs.

EXPERIMENTAL

Materials

Cotton was harvested from Xinjiang province, PR China. The cotton fiber was separated from the seed by rolling mill and was used as the raw cotton material. Analytical grade sulfuric acid was purchased from Beijing Chemical Factory (Beijing, China). The content of sulfuric acid was 95% to 98%. Deionized water (3 μS cm^{-1}) was prepared with a Heal force Water Purification System (Shanghai, China).

Sulfuric Acid Hydrolysis of Cellulose

First, 10 g raw cotton fiber was added to a 500 mL beaker containing 200 mL of 64.1% (w/w) sulfuric acid. To investigate the effects of pre-mixing time at room temperature on the yield and properties of CNCs, the mixture was stirred at 100 rpm with a magnetic rotor for 0, 30, 60, 120, and 180 min. The beaker was transferred to a water bath at 45 °C for 60 min. Immediately following the acid hydrolysis, the suspension was diluted with 10-fold deionized water to quench the reaction. To remove the unreacted cotton fiber and some leaves, the solution was passed through nylon filters of 100-mesh and 500 mesh. The suspension was centrifuged at 10,000 rpm for 10 min to concentrate the cellulose and remove excess aqueous acid. The resultant CNCs precipitate was rinsed, re-centrifuged three times, and dialyzed against water for one week until the electrical conductivity outside the dialysis bag was below 10 μS cm^{-1}. The resultant CNCs aqueous suspension was approximately 3% to 5% by weight. The produced CNCs with pre-mixing times of 0, 30, 60, 120, and 180 min were coded as CNC0, CNC30, CNC60, CNC120, CNC180, respectively. A 15 mL CNCs aqueous suspension was freeze dried for analysis.

Film Preparation

Approximately 10 mL of a CNCs aqueous suspension (~3 wt%) was added to the vacuum filtration apparatus mounted with a 0.22 μm PTFE membrane. After pumping for 8 h, the CNCs film had formed on the PTFE membrane and had a smooth surface. A micrometer was used to measure the thickness of the film. The yield of CNCs was obtained by weight from both the lyophilized sample and the film. The production process is illustrated in Fig. 1.

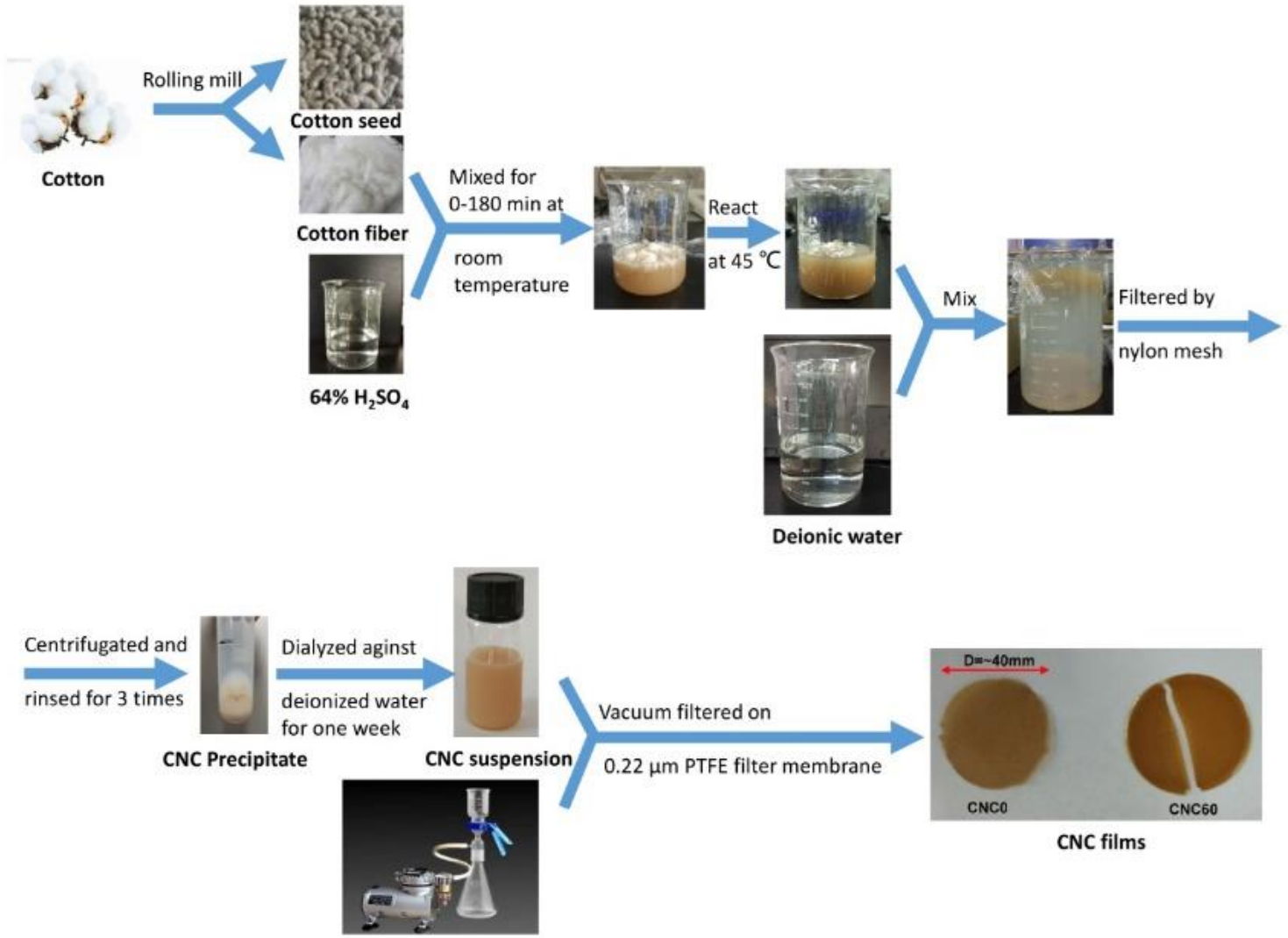

Fig. 1. The production process of CNC suspension and films with different pre-mixing times

CNCs Characterizations

Transmission electron microscopy

Drops of 0.001 wt.% CNC suspensions were deposited on glow-discharged carbon-coated copper grids (300 mesh). The specimens were then negatively stained with 1% phosphotungstic acid and observed using a Philips CM200 transmission electron microscope (TEM; Philips, Netherlands) operating at 80 kV. For each CNCs sample, the width and length of about 100 particles were measured from the TEM images using the Image J 1.46r software (https://imagej.nih.gov/ij/index.html).

X-ray diffraction (XRD) analysis

X-Ray diffraction measurements were conducted using a Panalytical X'Pert PRO MPD (Karlsruhe, Germany). The diffracted intensity of the Cu Kα radiation (0.154 nm, 40 kV, and 40 mA) was measured in a 2θ range between 10° and 50°. The CNCs films samples were characterized, and the crystallinity index (CrI) was determined by an empirical method using the following equation (Segal *et al.* 1959),

$$CrI(\%)=(I_{002}-I_{am})/I_{002}\times 100 \quad (1)$$

where I_{002} is the maximum intensity of the (002) lattice diffraction peak and I_{am} is the intensity scattered by the amorphous part of the sample. The diffraction peak for the plane (002) is located at a diffraction angle of around 2θ = 22.7°, and the intensity scattered by the amorphous part was measured as the lowest intensity at a diffraction angle of around 2θ = 18.7°.

Fourier transform infrared (FT-IR) spectroscopy

Fourier transform infrared spectroscopy was carried out on an FT-IR spectrophotometer (TENSOR II, Bruker Optics, Karlsruhe, Germany) using the KBr disk method. Before testing, the raw cotton fiber or CNCs was dried at 60 °C for 24 h and then ground in an agate mortar with KBr. The mass ratio between the sample and the dried KBr was 1:300. Thirty-two scans were carried out of each sample recorded from a range of 4000 cm^{-1} to 400 cm^{-1} at a resolution of 4 cm^{-1} in the transmission mode.

Thermogravimetric analysis (TGA)

The thermal stability of the CNCs was characterized using thermogravimetric analysis on a Shimadzu DTG-60 instrument (Kyoto, Japan). The samples (~ 5 mg) were heated from room temperature to 800 °C at a rate of 10 °C min^{-1} under a nitrogen flow rate of 50 mL min^{-1}.

Measurement of contact angle

The contact angle (CA) of the CNCs films with deionized water was measured using the dynamic contact angle meter (KINO SL200KS, KINO Industrial company ltd., City, America) mounted with CAST2.0 software (KINO Industrial Co., Ltd., America).

Birefringence of CNCs suspension

Approximately 0.2 mL of the CNCs suspension was injected into a rectangular vessel with a length of 40 mm, width of 10 mm, and a thickness of 1 mm. This vessel was ultra-sounded for 20 min at room temperature. Then this vessel was observed by a crossed polarizing microscope (model 58XC, Shanghai Optical Instrument Factory, Shanghai, China).

RESULTS AND DISCUSSION

Particle Morphology and Yield Analysis

Transmission electron microscopy (TEM) images of CNCs prepared by pre-mixing for 0 min and 60 min at room temperature prior to the reaction at 45 °C are shown in Fig. 2. The CNCs had a needle-like shape. The lengths and widths were obtained by measuring more than 100 individual CNCs rods in several images, as listed in the statistic results in Table 1 and Fig. 3. The length and width of the CNC60 was lower than those of CNC0. This result suggests that longer time spent by the mixed cotton with sulfuric acid resulted in smaller CNCs (Jiang and Hsieh 2013; Chen *et al.* 2015). In the case of CNCs produced from Whatman filter paper, Dong *et al.* (1998) showed that the length of the nanocrystals steadily decreased from 390 nm to 177 nm as the hydrolysis time increased from 10 min to 240 min (Dong *et al.* 1998). The standard deviation of distributions of length and width of CNC60 also decreased. Similar results were reported by Beck-Candanedo *et al.* (2005). The CNC60 had a more uniform dimension than CNC0. In CNC180, no needle-like shape was found.

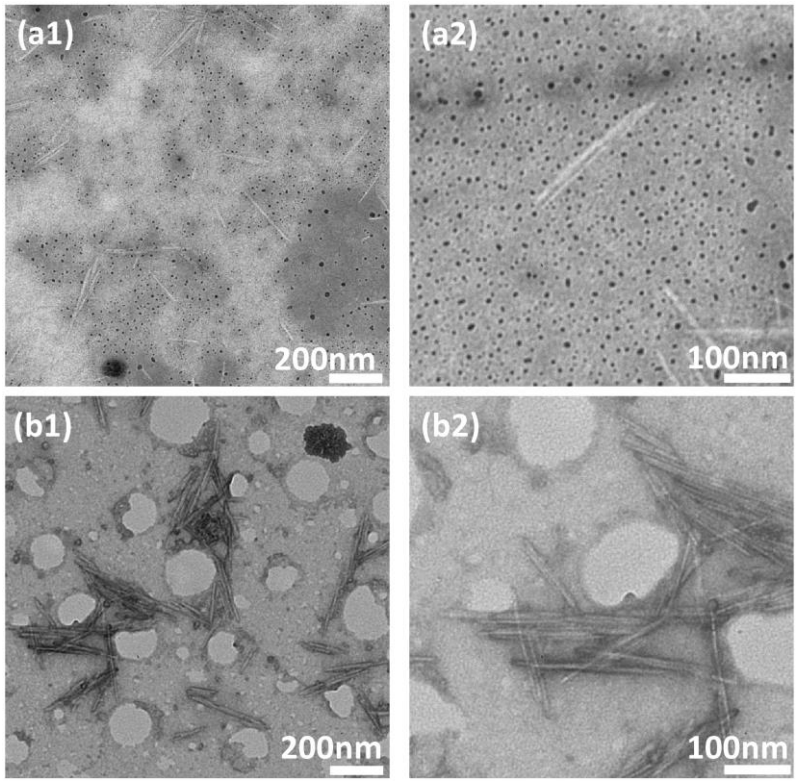

Fig. 2. TEM images of CNCs prepared by pre-mixing for 0 min (CNC0, a1 and a2) and 60 min (CNC60, b1 and b2) at room temperature.

Table 1. Statistics of Dimensions of CNC0 and CNC60

Sample Codes	Length					Width					Aspect ratio
	Mean	SD	RSD	Min	Max	Mean	SD	RSD	Min	Max	
CNC0	145	76	52.2%	35	405	7.7	2.3	30.4%	4.0	13.6	18.9
CNC60	137	58	42.8%	43	323	7.1	1.7	24.5%	3.5	13.5	19.2

Note: Error of measurement of length and width in TEM images is 7 nm and 0.6 nm, respectively

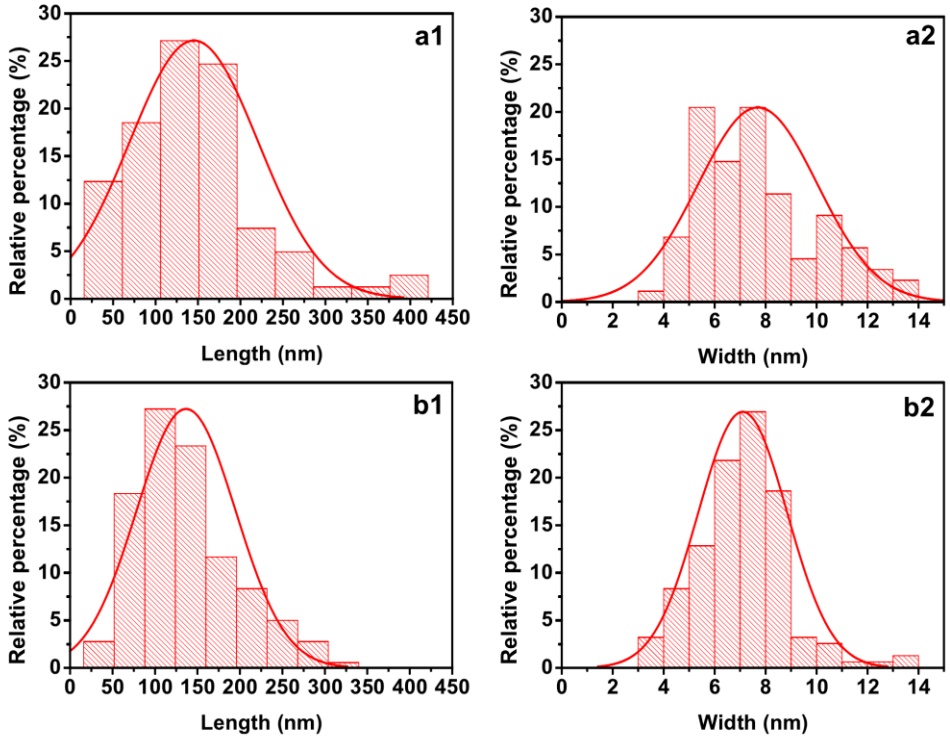

Fig. 3. Distribution of length and width of CNC0 (a1 and a2) and CNC60 (b1 and b2).

The yield values of various CNCs are shown in Table 2 and Fig. 4. The yield of CNC dropped drastically from CNC0 to CNC60, by 17.0% to 4.2%. This trend is consistent with previously reported results (Bondeson *et al.* 2006; Kargarzadeh *et al.* 2012; Wang *et al.* 2012; Jiang and Hsieh 2013). The yields of CNCs and preparation methods in the literature are summarized in Table 3. The CNCs yield of this work is close to the value of Jiang and Hsieh (2013) and Salminen *et al.* (2017). This may be due to the difference of condition during the preparation of CNCs. Considering the balance of yield and quality of CNCs, CNC0 was chosen as the optimum product in this paper.

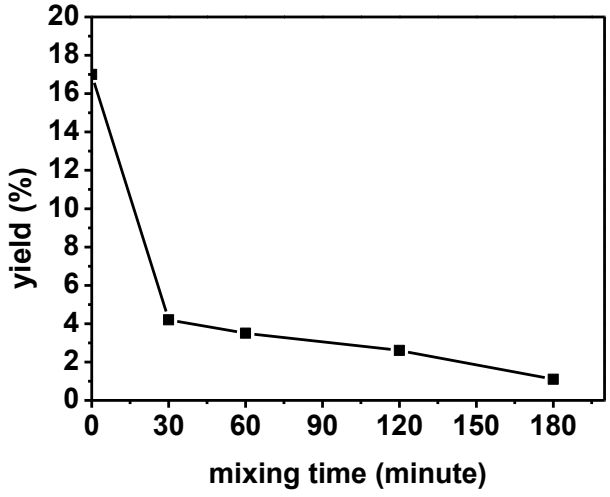

Fig. 4. The relationship between yield and pre-mixing time at room temperature

Table 2. Yield of CNCs using Different Pre-mixing Time at Room Temperature

Sample Codes	CNC0	CNC30	CNC60	CNC120	CNC180
Yield (%)	17.0	4.2	3.5	2.6	1.1

Table 3. Yield of CNCs and Preparation Conditions in the Literature and This Work

Raw material	method	Hydrolysis temperature/°C	Hydrolysis time/min	Solid:liquid ratio	CNC yield/%	Reference
Bleached kraft wood pulp	Sulfuric acid , 65%	70	30	1:10	50-60	Revol *et al.* 1992
Cotton-based filter paper powder	Sulfuric acid , 64%	26-65	10-240	1:8.75	34-48	Dong *et al.* 1998
MCC	Sulfuric acid , 63.5%	44.0	130.3	1:10.2	30	Bondeson *et al.* 2006
Cellulose extracted from kenaf bast fiber	Sulfuric acid , 65%	45	40	Not Mentioned	41	Kargarzadeh *et al.* 2012
Bleached Kraft eucalyptus dry lap pulp	Sulfuric acid , 58%	56	100	1:8, Stirring , 200 rpm	55.7	Wang *et al.* 2012
MCC	Sulfuric acid , 57-60%	45-55	40-60	1:8-10	70-75	Ioelovich 2012a
MCC	Sulfuric acid , 57-60%	45	60	1:10	65-70	Ioelovich 2012b
Pure cellulose isolated from rice straw	Sulfuric acid , 64%	45	60	1:8.75	16.9	Jiang and Hsieh 2013
MCC, cotton and pulp	6 mol/L HCl aqueous solutions under hydrothermal conditions	110	180	1:16667(60mg /L)	93.7	Yu *et al.* 2013
Bleached kraft eucalyptus pulp	Sulfuric acid , 58%	55	180	Not Mentioned	70	Wang *et al.* 2014
Bleached kraft eucalyptus pulp	Sulfuric acid , 58%	35-80	15-240	1:10	70	Chen *et al.* 2015
Softwood sulfite pulp	Sulfuric acid , 64%, and ultrasound	45	120	1:15	71.0	Guo *et al.* 2016
Cotton-based filter paper	Hydrogen Chloride Vapor hydrolysis	Room temperature	60	none	97.4	Kontturi *et al.* 2016
MCC	TEMPO-mediated oxidation	Room temperature	~30	Not Mentioned	17–20	Salminen *et al.* 2017
Cotton-based filter paper	TEMPO-mediated oxidation after hydrolysis by HCl vapour	Room temperature	hydrolysis for 12 h	none	50	Lorenz *et al.* 2017
Raw cotton	Sulfuric acid , 64.1%	45	60	1:20	17.0	This work

The interaction between cotton fibers and sulfuric acid can be divided into two sequential processes, specifically that of the solubilization and the depolymerization of cellulose. As reported by Camacho *et al*. (1996) and Wang *et al*. (2014), these two processes have different kinetics. At 45 °C, the kinetic constant, *k*, in the solubilization depolymerization process would be about ten times that of *k* at 25 °C (Camacho *et al.* 1996). The reaction rate at 45 °C would be about ten times that of the rate at 25 °C. However, in this paper, along with the increased pre-mixing time at 25 °C, the yield decreased remarkably. This means that the process at 25 °C played an important role in the production of CNCs, which could be comparable with that at 45 °C. Therefore, the two processes should be more complicated than the results of Camacho *et al*. (1996) and Wang *et al*. (2014).

X-ray Diffraction Analysis

XRD experiments were conducted to analyze the crystallinity of various CNCs. The XRD patterns for CNC0 and CNC60 films are shown in Fig. 5. All diffractograms were typical of semi-crystalline materials, displaying an amorphous broad hump and crystalline peaks. As shown in Table 4, four well-defined crystalline peaks of cellulose I were present at 2θ = 14.8°, 16.8°, 22.8°, and 34.3° (Kargarzadeh *et al.* 2017).

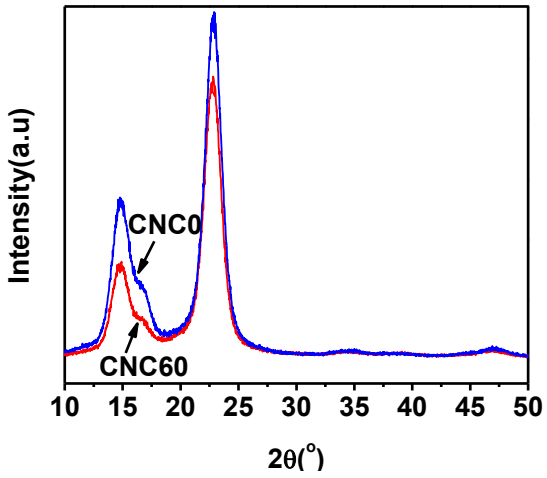

Fig. 5. X-ray diffraction patterns of CNC0 and CNC60 films prepared by vacuum filtration

Table 4. Diffraction Peak, Crystallinity Index, and Thickness of CNC0 and CNC60 Films

Sample Codes	Peak 1 Position	Peak 2 Position	Peak 3 Position	Peak 4 Position	Peak 5 Position	CrI (%)	Film Thickness (μm)
CNC0	14.8	16.8	22.9	34.3	46.9	92.5	173
CNC60	14.8	16.8	22.8	34.3	46.9	92.6	137μm

The crystallinity indexes (CrI) determined from these diffractograms are shown in Table 4. The CrI was 92.5% for CNC0. The CrI value of raw cotton was approximately 79.2% (Segal *et al.* 1959). Thus, after the acid hydrolysis treatment, the CrI value increased. This finding confirms that the cellulosic amorphous polysaccharides were efficiently removed using the acid treatment. The CrI value increased little upon the increase of pre-mixing time at room temperature from 0 min to 60 min. This result indicated

that the amorphous region of cotton fiber had been removed completely. It should be noted that the peak intensities of CNC60 were lower than that of the corresponding peaks of CNC0, indicating the decreased crystallinity (Liu *et al.* 2008).

FT-IR Analysis

Figure 6 displays the FT-IR spectra of raw cotton and five kinds of CNCs. The band at 3350 cm^{-1} is the O-H stretching vibration peak. The bands at 2918 cm^{-1} and 2851 cm^{-1} are the C-H peaks. The band at 1636 cm^{-1} is the bending vibration peak of water. The band at 1372 cm^{-1} is the bending vibration peak of C-H. The bands at 1162, 1112, 1060, and 1034 cm^{-1} are the peaks of C-O-C-O-C (Suflet *et al.* 2006). The band at 898 cm^{-1} is related to the C–H rocking vibration (Alemdar and Sain 2008), which is the characteristic absorption of cellulose. The band at 614 cm^{-1} is the fingerprint absorption of a hexatomic ring in carbohydrate. Hence, there is little difference among these FT-IR spectra, which is the consequence of the similar chemical structure of various CNCs.

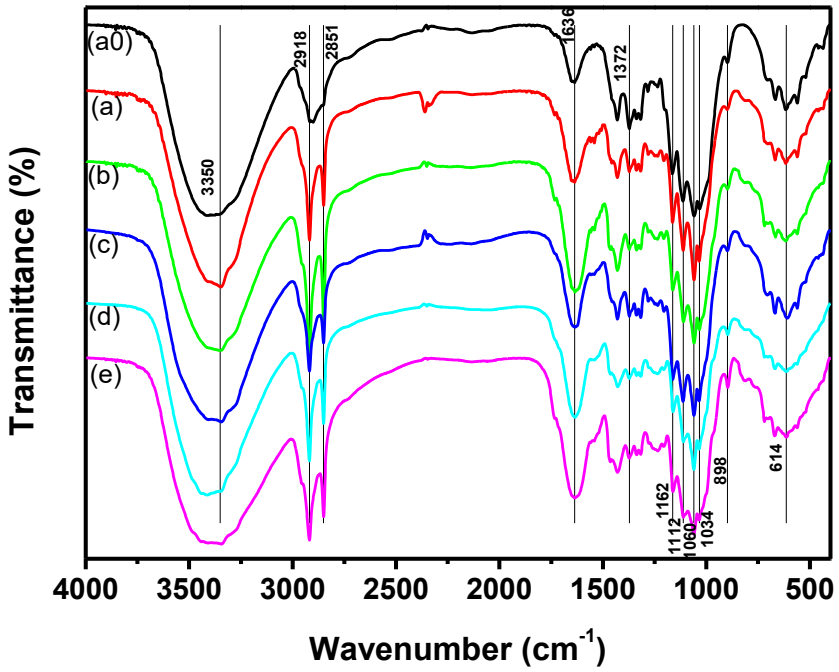

Fig. 6. FT-IR spectra of raw cotton (a0) and five kinds of CNCs under different pre-mixing time: (a) 0 min; (b) 30 min; (c) 60 min; (d) 120 min; (e) 180 min

Thermogravimetric Analysis

The TG and DTG curves of the raw cotton materials and the three kinds of CNCs produced under different pre-mixing times are shown in Fig. 7. There are several overlapping peaks in the curves. Peakfit 4.0 software was used to deconvolute the DTG curves (Roman and Winter 2004). The CNCs codes, center values, temperature ranges, and areas of deconvoluted peaks are listed in Tables 5 through 7, respectively. The raw cotton has three peak codes at 1, 4, and 5. Peak 1 centered at 66.4 °C corresponded to the evaporation of water. Peak 4 centered at 340.7 °C corresponded to the pyrolysis of cellulose and has a similar position and temperature range (Broido 1969; Yang *et al.* 2007). Peak 5 centered at 411.6 °C had the largest temperature range of the three peaks. This maybe

corresponded to charring process of solid residues reported by Wang *et al.* (2007). Cotton fibers usually have a cellulose content of more than 80 wt.% (Zhang *et al.* 2012). In these three peaks, peak 4 had the maximum area ratio of 95%, indicating that raw cotton contained mostly cellulose.

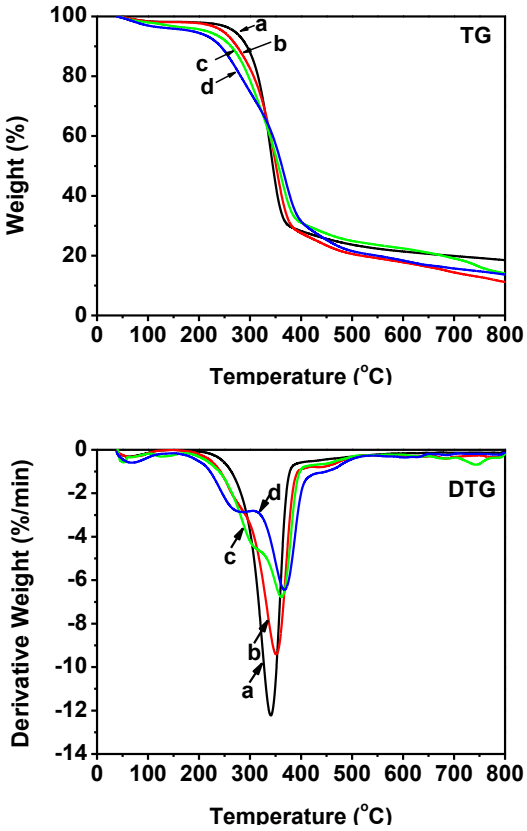

Fig. 7. TG and DTG curves of raw cotton (a) and three kinds of CNCs: (b) CNC0; (c) CNC60; (d) CNC180

These three peaks also appeared in three kinds of CNCs around a similar position and would represent similar chemical components as seen in raw cotton. CNC0 had two more peaks than raw cotton, and both the CNC60 and CNC180 also had some changes in their peaks in comparison to the CNC0. These changes of peaks can be observed in Table 5. Because peaks 3, 4, and 5 had higher area ratios than others, and the analysis of peaks 2 and 6 was difficult due to its low content. Only the changes of peaks 3, 4, and 5 are discussed in relation to these samples. Peak 3 should be ascribed to the pyrolysis of cellulose catalyzed by sulfated groups at the surface of the CNCs (Roman and Winter 2004; Man *et al.* 2011). By increasing the pre-mixing time at room temperature, the area ratio of peak 3 increased gradually from 15% to 30%, and the area ratio of peak 4 decreased from 75% to 56%. In considering the results of XRD, CNCs had similar CrI values for various CNCs. After conductometric titration were carried out on CNC0 and CNC60, the contents of sulfate groups were 89 and 214 mmol/kg, respectively. One can see the increased sulfate group along with the increase of pretreatment time. Further, this caused the changes of the area ratio of peaks 3 and 4. We proposed the possible mechanism to explain the increase thermal degradation with acid treatment. The degradation of cellulose catalyzed by sulfuric

acid would cause more char residues (Kim *et al.* 2001; Roman and Winter 2004; Wang *et al.* 2007). These char residues covered the surface of CNC and slowed the heat transfer of CNC, delaying the pyrolysis of CNC (Simmons and Gentry 1986).

The color of CNC0 and CNC60 was claybank, and the color of CNC60 was deeper than that of CNC0 (Fig. 1). The commercial CNCs have a white color and by tedious sediment separation steps, white CNCs were obtained from this experiment also. The claybank color may be due to the existence of impurities in the products. These impurities might be the small molecules of xylan, lactic acid, and levulinic acid, etc, during acid hydrolysis procedure (Labet and Thielemans 2011). In combination with the gradually decrease yield of CNCs, one can understand the increase of the relative content of impurities.

Table 5. Centered Value of Peaks in Deconvoluted DTG Curves of Raw Cotton and CNCs

Sample Code	Temperature (°C)					
	Peak 1	Peak 2	Peak 3	Peak 4	Peak 5	Peak 6
raw cotton	66.4	-	-	340.7	411.6	-
CNC0	68.5	-	294.3	350.5	449.7	683.0
CNC60	61.0	125.5	303.9	360.2	431.4	743.8
CNC180	73.1	-	277.2	368.4	448.5	594.8

Table 6. Temperature Range of Peaks in Deconvoluted DTG Curves of Raw Cotton and CNCs

Sample Code	Temperature Range (°C)					
	Peak 1	Peak 2	Peak 3	Peak 4	Peak 5	Peak 6
raw cotton	26.0-106.8	-	-	294.1-387.3	321.9-501.3	-
CNC0	28.3-108.7	-	218.6-370.0	304.4-396.6	393.9-505.5	646.5-719.5
CNC60	2.1-119.9	69.5-181.5	237.4-370.4	309.3-411.1	322.3-540.5	698.8-788.8
CNC180	26.3-119.9	-	199.6-354.8	312.6-424.2	361.5-535.5	456.0-733.6

Table 7. Area Ratio of Peaks in Deconvoluted DTG Curves of Raw Cotton and CNCs

Sample Code	Area Ratio (%)					
	Peak 1	Peak 2	Peak 3	Peak 4	Peak 5	Peak 6
raw cotton	2	-	-	95	4	-
CNC0	3	-	15	75	6	1
CNC60	6	2	29	51	8	4
CNC180	3	-	30	56	10	2

Contact Angle Analysis

The images of contact angles (CA) of CNCs films are shown in Fig. 8. The CA values of CNCs films are listed in Table 8. By increasing the pre-mixing time, the CA decreased from 56.19° to 46.65°. This result suggested that the hydrophilicity of CNCs increased. The increased CA could be the result of a decrease in dimension of CNCs or the increase of sulfate groups at the surface of CNCs.

Fig. 8. Images of CA of CNC0 and CNC60 films

Table 8. Contact Angle of CNCs Films

Film name	Contact angle (°)
CNC0	56.19
CNC60	46.46

Birefringence of CNCs Suspension

The fingerprint-like textures of CNCs suspensions were observed by a polarizing microscope, as shown in Fig. 9. The micrograph shows that the half pitch of chiral nematic ordered phase was 7 μm to 18 μm. This observation, in addition to the reported results (Revol *et al.* 1992), verified the successful production of CNCs.

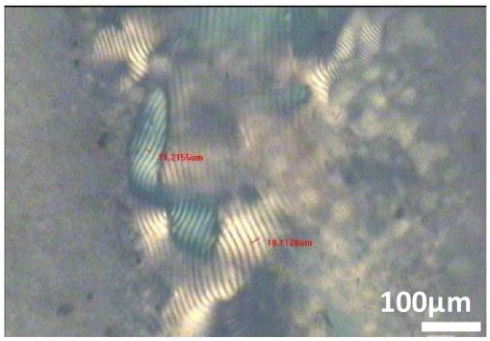

Fig. 9. The fingerprint-like multi-domains formed in the CNC's suspension shows a half pitch of 7 8 μm to 18 μm

CONCLUSIONS

1. Cellulose nanocrystals (CNCs) were produced using different pre-mixing times between the cotton fiber and the sulfuric acid at room temperature prior to a reaction at 45 °C. It was concluded that the dimension of CNCs was gradually decreased, in a uniform manner, with the increasing pre-mixing time. The yield of CNCs decreased, too.
2. The process at 25 °C played an important role in the production of CNCs, indicating that the dependence of the two processes on temperature should be more complex.

3. The CNC0 and CNC60 films were prepared using a vacuum filtration method. When XRD was carried out on these films, it was demonstrated that the crystalline polymorph of cellulose I was maintained.
4. From the result of the FT-IR and TG, the main constituents of various CNCs were verified to be cellulose. Besides this, the quantities of sulfate groups in the surface of CNCs increased gradually from CNC0 to CNC60.
5. The decrease of contact angle (CA) of water was the result of the decreased dimension of CNCs or the increase of sulfate groups on the surface of the CNCs. CA is an indirect method used to indicate the relative dimensions of CNCs.

ACKNOWLEDGMENTS

This project was financially supported by the Fundamental Research Funds for the Central Universities (No. 2017ZY49) and the Young Teachers Cultivating Scientific Research Project (No. XJEDU2016S042) of University Scientific Research Plan of Xinjiang Uygur Autonomous Region.

REFERENCES CITED

Alemdar, A., and Sain, M. (2008). "Isolation and characterization of nanofibers from agricultural residues - Wheat straw and soy hulls," *Bioresource Technol.* 99(6), 1664-1671. DOI: 10.1016/j.biortech.2007.04.029

Beck-Candanedo, S., Roman, M., and Gray, D. G. (2005). "Effect of reaction conditions on the properties and behavior of wood cellulose nanocrystal suspensions," *Biomacromolecules* 6(2), 1048-1054. DOI: 10.1021/bm049300p

Biyani, M. V., Foster, E. J., and Weder, C. (2013). "Light-healable supramolecular nanocomposites based on modified cellulose nanocrystals," *ACS Macro Lett.* 2(3), 236-240. DOI: 10.1021/mz400059w

Biyani, M. V., Jorfi, M., Weder, C., and Foster, E. J. (2014). "Light-stimulated mechanically switchable, photopatternable cellulose nanocomposites," *Polym. Chem.* 5(19), 5716-5724. DOI: 10.1039/c4py00487f

Bondeson, D., Mathew, A., and Oksman, K. (2006). "Optimization of the isolation of nanocrystals from microcrystalline cellulose by acid hydrolysis," *Cellulose* 13(2), 171-180. DOI: 10.1007/s10570-006-9061-4

Broido, A. (1969). "Simple, sensitive graphical method of treating thermogravimetric analysis data," *J. Polym. Sci.: Part A-2* 7(10), 1761-1773.

Camacho, F., González-Tello, P., Jurado, E., and Robles, A. (1996). "Microcrystalline-cellulose hydrolysis with concentrated sulphuric acid," *J. Chem. Technol. Biotechnol.* 67(4), 350-356. DOI: 10.1002/(SICI)1097-4660(199612)67:4

Chen, L. H., Wang, Q. Q., Hirth, K., Baez, C., Agarwal, U. P., and Zhu, J. Y. (2015). "Tailoring the yield and characteristics of wood cellulose nanocrystals (CNC) using concentrated acid hydrolysis," *Cellulose* 22(3), 1753-1762. DOI: 10.1007/s10570-015-0615-1

Chieng, B. W., Lee, S. H., Ibrahim, N. A., Then, Y. Y., and Loo, Y. Y. (2017). "Isolation and characterization of cellulose nanocrystals from oil palm mesocarp fiber,"

Polymers 9(8), 355. DOI: 10.3390/polym9080355

Csiszar, E., and Nagy, S. (2017). "A comparative study on cellulose nanocrystals extracted from bleached cotton and flax and used for casting films with glycerol and sorbitol plasticisers," *Carbohyd. Polym.* 174, 740-749. DOI: 10.1016/j.carbpol.2017.06.103

Dong, X. M., Revol, J. F., and Gray, D. G. (1998). "Effect of microcrystallite preparation conditions on the formation of colloid crystals of cellulose," *Cellulose* 5(1), 19-32. DOI: 10.1023/a:1009260511939

Elazzouzi-Hafraoui, S., Nishiyama, Y., Putaux, J. L., Heux, L., Dubreuil, F., and Rochas, C. (2008). "The shape and size distribution of crystalline nanoparticles prepared by acid hydrolysis of native cellulose," *Biomacromolecules* 9(1), 57-65. DOI: 10.1021/bm700769p

Fortunati, E., Armentano, I., Zhou, Q., Iannoni, A., Saino, E., Visai, L., Berglund, L. A., and Kenny, J. M. (2012). "Multifunctional bionanocomposite films of poly(lactic acid), cellulose nanocrystals and silver nanoparticles," *Carbohydr. Polym.* 87(2), 1596-1605. DOI: 10.1016/j.carbpol.2011.09.066

Gawryla, M. D., van den Berg, O., Weder, C., and Schiraldi, D. A. (2009). "Clay aerogel/cellulose whisker nanocomposites: A nanoscale wattle and daub," *J. Mater. Chem.* 19(15), 2118-2124. DOI: 10.1039/b823218k

Guo, J., Guo, X., Wang, S., and Yin, Y. (2016). "Effects of ultrasonic treatment during acid hydrolysis on the yield, particle size and structure of cellulose nanocrystals," *Carbohydr. Polym.* 135, 248-255. DOI: 10.1016/j.carbpol.2015.08.068

Habibi, Y., Lucia, L. A., and Rojas, O. J. (2010). "Cellulose nanocrystals: Chemistry, self-assembly, and applications," *Chem. Rev.* 110(6), 3479-3500. DOI: 10.1021/cr900339w

Huang, B., Lu, Q. L., and Tang, L. R. (2016). "Research progress of nanocellulose manufacture and application," *J. Forestry Engineer.* 1(05), 1-9.

Imato, K., Natterodt, J. C., Sapkota, J., Goseki, R., Weder, C., Takahara, A., and Otsuka, H. (2017). "Dynamic covalent diarylbibenzofuranone-modified nanocellulose: Mechanochromic behaviour and application in self-healing polymer composites," *Polym. Chem.* 8(13), 2115-2122. DOI: 10.1039/c7py00074j

Ioelovich, M. (2012a). "Optimal conditions for isolation of nanocrystalline cellulose particles," *Nanosciand. Nanotechno.* 2(2), 9-13. DOI: 10.5923/j.nn.20120202.03

Ioelovich, M. (2012b). "Study of cellulose interaction with concentrated solutions of sulfuric acid," *ISRN Chem. Engineer.* Article Number 428974. DOI: 10.5402/2012/428974

Ioelovich, M. (2016). "Products of cellulose hydrolysis made by treatment of feedstock with concentrated solutions of sulfuric acid," *Res. Rev.: J. Mater. Sci.* 01(01). DOI: 10.4172/2321-6212.1000103

Jiang, F., and Hsieh, Y. L. (2013). "Chemically and mechanically isolated nanocellulose and their self-assembled structures," *Carbohyd. Polym.* 95(1), 32-40. DOI: 10.1016/j.carbpol.2013.02.022

Kargarzadeh, H., Ahmad, I., Abdullah, I., Dufresne, A., Zainudin, S. Y., and Sheltami, R. M. (2012). "Effects of hydrolysis conditions on the morphology, crystallinity, and thermal stability of cellulose nanocrystals extracted from kenaf bast fibers," *Cellulose* 19(3), 855-866. DOI: 10.1007/s10570-012-9684-6

Kargarzadeh, H., Ahmad, I., Thomas, S., and Dufresne, A. (2017). *Handbook of Nanocellulose and Cellulose Nanocomposites*, Wiley-VCH Verlag, Weinheim,

Germany.

Kim, D. Y., Nishiyama, Y., Wada, M., and Kuga, S. (2001). "High-yield carbonization of cellulose by sulfuric acid impregnation," *Cellulose* 8(1), 29-33. DOI: 10.1023/A:1016621103245

Kontturi, E., Meriluoto, A., Penttila, P. A., Baccile, N., Malho, J. M., Potthast, A., Rosenau, T., Ruokolainen, J., Serimaa, R., Laine, J., and Sixta, H. (2016). "Degradation and crystallization of cellulose in hydrogen chloride vapor for high-yield isolation of cellulose nanocrystals," *Angew. Chem. Int. Ed.* 55(46), 14455-14458. DOI: 10.1002/anie.201606626

Labet, M., and Thielemans, W. (2011). "Improving the reproducibility of chemical reactions on the surface of cellulose nanocrystals: ROP of epsilon-caprolactone as a case study," *Cellulose* 18(3), 607-617. DOI: 10.1007/s10570-011-9527-x

Lee, K.-Y. (2018). "Preparation of cellulose nanocrystals: Background, conventions and new developments," in: *Nanocellulose and Sustainability: Production, Properties, Applications, and Case Studies*, CRC Press, Boca Raton, EBook ISBN: 9781351262910

Li, C., Li, Q. D., Ni, X. H., Liu, G. X., Cheng, W. L., and Han, G. P. (2017). "Coaxial electrospinning and characterization of core-shell structured cellulose nanocrystal reinforced PMMA/PAN composite fibers," *Materials* 10(6), 16. DOI: 10.3390/ma10060572

Liu, S. L., Zhang, L., Zhou, J. P., and Wu, R. X. (2008). "Structure and properties of cellulose/Fe_2O_3 nanocomposite fibers spun via an effective pathway," *J. Phys. Chem. C* 112(12), 4538-4544. DOI: 10.1021/jp711431h

Lorenz, M., Sattler, S., Reza, M., Bismarck, A., and Kontturi, E. (2017). "Cellulose nanocrystals by acid vapour: Towards more effortless isolation of cellulose nanocrystals," *Faraday Discuss.* 202, 315-330. DOI: 10.1039/c7fd00053g

Man, Z., Muhammad, N., Sarwono, A., Bustam, M. A., Kumar, M. V., and Rafiq, S. (2011). "Preparation of cellulose nanocrystals using an ionic liquid," *J. Polym. Environ.* 19(3), 726-731. DOI: 10.1007/s10924-011-0323-3

Meesorn, W., Shirole, A., Vanhecke, D., de Espinosa, L. M., and Weder, C. (2017). "A simple and versatile strategy to improve the mechanical properties of polymer nanocomposites with cellulose nanocrystals," *Macromolecules* 50(6), 2364-2374. DOI: 10.1021/acs.macromol.6b02629

Mendez, J., Annamalai, P. K., Eichhorn, S. J., Rusli, R., Rowan, S. J., Foster, E. J., and Weder, C. (2011). "Bioinspired mechanically adaptive polymer nanocomposites with water-activated shape-memory effect," *Macromolecules* 44(17), 6827-6835. DOI: 10.1021/ma201502k

Moon, R. J., Martini, A., Nairn, J., Simonsen, J., and Youngblood, J. (2011). "Cellulose nanomaterials review: structure, properties and nanocomposites," *Chem. Soc. Rev.* 40(7), 3941-3994. DOI: 10.1039/c0cs00108b

Mukherjee, S. M., and Woods, H. J. (1953). "X-ray and electron microscope studies of the degradation of cellulose by sulphuric acid," *Biochim. Biophys. Acta* 10(4), 499-511. DOI: 10.1016/0006-3002(53)90295-9

Nicharat, A., Shirole, A., Foster, E. J., and Weder, C. (2017). "Thermally activated shape memory behavior of melt-mixed polyurethane/cellulose nanocrystal composites," *J. Appl. Polym. Sci.* 134(27), 10. DOI: 10.1002/app.45033

Padalkar, S., Capadona, J. R., Rowan, S. J., Weder, C., Won, Y. H., Stanciu, L. A., and Moon, R. J. (2010). "Natural biopolymers: Novel templates for the synthesis of

nanostructures," *Langmuir* 26(11), 8497-8502. DOI: 10.1021/la904439p

Pei, A. H., Malho, J. M., Ruokolainen, J., Zhou, Q., and Berglund, L. A. (2011). "Strong nanocomposite reinforcement effects in polyurethane elastomer with low volume fraction of cellulose nanocrystals," *Macromolecules* 44(11), 4422-4427. DOI: 10.1021/ma200318k

Rånby, B. G. (1951). "Fibrous macromolecular systems. Cellulose and muscle. The colloidal properties of cellulose micelles," *Discuss. Faraday Soc.* (11), 158-164.

Revol, J. F., Bradford, H., Giasson, J., Marchessault, R. H., and Gray, D. G. (1992). "Helicoidal self-ordering of cellulose microfibrils in aqueous suspension," *Int. J. Biol. Macromol.* 14(3), 170-172. DOI: 10.1016/s0141-8130(05)80008-x

Roman, M., and Winter, W. T. (2004). "Effect of sulfate groups from sulfuric acid hydrolysis on the thermal degradation behavior of bacterial cellulose," *Biomacromolecules* 5(5), 1671-1677. DOI: 10.1021/bm034519+

Salminen, R., Reza, M., Paakkonen, T., Peyre, J., and Kontturi, E. (2017). "TEMPO-mediated oxidation of microcrystalline cellulose: Limiting factors for cellulose nanocrystal yield," *Cellulose* 24(4), 1657-1667. DOI: 10.1007/s10570-017-1228-7

Sampath, U., Ching, Y., Chuah, C., Singh, R., and Lin, P. (2017). "Preparation and characterization of nanocellulose reinforced semi-interpenetrating polymer network of chitosan hydrogel," *Cellulose* 24(5), 2215-2228.DOI: 10.1007/s10570-017-1251-8

Sapkota, J., Natterodt, J. C., Shirole, A., Foster, E. J., and Weder, C. (2017). "Fabrication and properties of polyethylene/cellulose nanocrystal composites," *Macromol. Mater. Engineer.* 302(1), 6. DOI: 10.1002/mame.201600300

Schyrr, B., Pasche, S., Voirin, G., Weder, C., Simon, Y. C., and Foster, E. J. (2014). "Biosensors based on porous cellulose nanocrystal-poly(vinyl alcohol) scaffolds," *ACS Appl. Mater. Interfaces* 6(15), 12674-12683. DOI: 10.1021/am502670u

Segal, L., Creely, J. J., Martin, A. E., Jr., and Conrad, C. M. (1959). "An empirical method for estimating the degree of crystallinity of native cellulose using the x-ray diffractometer," *Text. Res. J.* 29(10), 786-794. DOI: 10.1177/004051755902901003

Shanmuganathan, K., Capadona, J. R., Rowan, S. J., and Weder, C. (2010). "Bio-inspired mechanically-adaptive nanocomposites derived from cotton cellulose whiskers," *J. Mater. Chem.* 20(1), 180-186. DOI: 10.1039/b916130a

Simmons, G. M., and Gentry, M. (1986). "Particle-size limitations due to heat-transfer in determining pyrolysis kinetics of biomass," *J. Analyt. Appl. Pyrolys.* 10(2), 117-127. DOI: 10.1016/0165-2370(86)85011-2

Sobolciak, P., Tanvir, A., Popelka, A., Moffat, J., Mahmoud, K. A., and Krupa, I. (2017). "The preparation, properties and applications of electrospun co-polyamide 6,12 membranes modified by cellulose nanocrystals," *Mater. Design* 132, 314-323. DOI: 10.1016/j.matdes.2017.06.056

Suflet, D. M., Chitanu, G. C., and Popa, V. I. (2006). "Phosphorylation of polysaccharides: New results on synthesis and characterisation of phosphorylated cellulose," *React. Funct. Polym.* 66(11), 1240-1249. DOI: 10.1016/j.reactfunctpolym.2006.03.006

Trache, D., Hussin, M. H., Haafiz, M. K. M., and Thakur, V. K. (2017). "Recent progress in cellulose nanocrystals: Sources and production," *Nanoscale* 9(5), 1763-1786. DOI: 10.1039/c6nr09494e

Wang, N., Ding, E. Y., and Cheng, R. S. (2007). "Thermal degradation behaviors of spherical cellulose nanocrystals with sulfate groups," *Polymer* 48(12), 3486-3493. DOI: 10.1016/j.polymer.2007.03.062

Wang, Q. Q., Zhao, X. B., and Zhu, J. Y. (2014). "Kinetics of strong acid hydrolysis of a bleached kraft pulp for producing cellulose nanocrystals (CNCs)," *Ind. Eng. Che. Res.* 53(27), 11007-11014. DOI: 10.1021/ie501672m

Wang, Q. Q., Zhu, J. Y., Reiner, R. S., Verrill, S. P., Baxa, U., and McNeil, S. E. (2012). "Approaching zero cellulose loss in cellulose nanocrystal (CNC) production: Recovery and characterization of cellulosic solid residues (CSR) and CNC," *Cellulose* 19(6), 2033-2047. DOI: 10.1007/s10570-012-9765-6

Way, A. E., Hsu, L., Shanmuganathan, K., Weder, C., and Rowan, S. J. (2012). "pH-responsive cellulose nanocrystal gels and nanocomposites," *ACS Macro Lett.* 1(8), 1001-1006. DOI: 10.1021/mz3003006

Yan, H. Q., Chen, X. Q., Song, H. W., Li, J. C., Feng, Y. H., Shi, Z. F., Wang, X. H., and Lin, Q. (2017). "Synthesis of bacterial cellulose and bacterial cellulose nanocrystals for their applications in the stabilization of olive oil pickering emulsion," *Food Hydrocolloid.* 72, 127-135. DOI: 10.1016/j.foodhyd.2017.05.044

Yu, H. Y., Qin, Z. Y., Liang, B. L., Liu, N., Zhou, Z., and Chen, L. (2013). "Facile extraction of thermally stable cellulose nanocrystals with a high yield of 93% through hydrochloric acid hydrolysis under hydrothermal conditions," *J. Mater. Chem. A* 1(12), 3938-3944. DOI: 10.1039/c3ta01150j

Yu, H.-Y., Wang, C., and Abdalkarim, S. Y. H. (2017). "Cellulose nanocrystals/ polyethylene glycol as bifunctional reinforcing/compatibilizing agents in poly(lactic acid) nanofibers for controlling long-term *in vitro* drug release," *Cellulose* 24(10), 4461-4477. DOI: 10.1007/s10570-017-1431-6

Zhang, M. L., Song, X. L., Sun, X. Z., Wang, Z. L., Li, Z. T., Ji, H., Xu, X. L., and Li, J. P. (2012). "The relationship between cellulose content and the contents of sugars and minerals during fiber development in colored cotton cultivars," *Cellulose* 19(6), 2003-2014. DOI: 10.1007/s10570-012-9776-3

Zhang, R. H., Zhang, W., Li, H., Ling, M., and Liu, Z. P. (2016). "Biopolyester P(3,4) HB-based nanocomposites reinforced by cellulose nanowhiskers," *Journal of Forestry Engineering* 1(03), 85-90.

Zhang, Y. Y., Wan, X., Mo, M. M., and Li, D. G. (2017). "Preparation of cellulose nanocrystal film and cholesteric liquid crystal pattern," *Journal of Forestry Engineering* 2(04), 103-108.

Article submitted: January 2, 2018; Peer review completed: February 17, 2018; Revised version received and accepted: March 23, 2018; Published: March 27, 2018.
DOI: 10.15376/biores.13.2.3585-3602